THE ASTROPHYSICAL JOURNAL, 330:274–285, 1988 July 1

PHYSICAL REALISM IN THE ANALYSIS OF STELLAR MAGNETIC FIELDS[1]

GIBOR BASRI
Astronomy Department, University of California, Berkeley
AND
GEOFFREY W. MARCY
Department of Physics and Astronomy, San Francisco State University
Received 1987 September 23; accepted 1987 December 22

ABSTRACT

We have reexamined the detection and analysis of magnetic fields on cool stars using improved theoretical and observational methods. We employ lines in the near-infrared which are both accessible at high signal-to-noise and resolution with CCD detectors, and more sensitive to Zeeman broadening than optical lines. We treat the analysis of these with a model atmosphere code which includes all relevant line and stellar physics (in LTE) instead of the approximate treatment of transfer that has been previously used. We carefully examine the possibility that observed broadenings could be due to deficiencies in past or present methods of analysis and conclude that magnetic fields are really being detected. In particular, for ϵ Eri we derive an average field strength of 1000 G covering 35% of the stellar surface and for ξ Boo A we derive a field of 1200 G covering 40% of the surface. We discuss in detail the analysis of fields from observations of spectral line profiles and mention some future improvements which could be made in it.

Subject headings: line profiles — stars: late-type — stars: magnetic — Zeeman effect

I. INTRODUCTION

One of the most compelling successes in stellar astrophysics during the past decade has been the establishment of a causal relationship between the strength of both chromospheric and coronal emission and the rotation rate of solar-type stars, e.g., Noyes *et al.* (1984), Simon and Fekel (1987), Basri (1987), Rutten and Schrijver (1987). The interpretation of this relationship, along with a better physical understanding of chromospheres and coronae themselves, requires knowledge of the processes by which the upper atmospheres of cool stars are thermally and structurally sustained. On the Sun, it is clear that the relevant processes involve the presence of magnetic fields. Thus, several efforts have been made recently to detect magnetic fields on other solar-type stars (Marcy 1984; Gray 1984*a*; Saar 1988*b*).

These studies all involve the detection of excess broadening of line profiles caused by the Zeeman effect, and all report that magnetic fields are present in the more chromospherically active stars. However, the reported increases in line breadth owing to the Zeeman effect are no more than a few percent. Thus the credibility of these magnetic-field detections hinges on the ability to detect and predict, with extreme accuracy, the shapes that the line profiles have if formed in the presence or absence of magnetic fields. Other attempts to measure the magnetic fields by directly detecting polarization suffer from the serious problem that the stellar surface is covered by opposite polarities, largely cancelling the polarization signal.

One method, proposed by Robinson (1980), is to compare, in the spectrum of a given star, the broadening of two lines having different Landé g-values, and thus different Zeeman sensitivities. This approach, employed by Robinson, Worden, and Harvey (1980), and Marcy (1984), has the drawback that, even in the absence of fields, the two observed lines may differ in shape owing to differences in gf-values, excitation, collisional broadening sensitivity, or blends. Robinson (1980) further proposed to derive magnetic field strengths and the fraction of the stellar surface covered by fields by modeling the observed Zeeman-broadened profile as the simple sum of three unbroadened profiles. While this approach is adequate for very weak lines, the errors incurred when applied to lines of moderate strength must be assessed very carefully.

Recently, Saar (1988*a*) has addressed some of these difficulties by using the known analytical solution to the equations of transfer of the four Stokes parameters in a simplified stellar atmosphere (Unno 1956). This calculation permits treatment of the polarized Zeeman absorption components and allows for different atomic parameters of the relevant transitions. Saar's work confirms the presence of magnetic fields on many G and K stars, and his results suggest that previous techniques may have systematically overestimated the fraction of the stellar surface covered by fields. This is because he has at least partially accounted for the effects of saturation in the line formation, which the original method does not.

The simplified atmosphere employed in Saar's work contains two major assumptions. The source function is taken to be linear with optical depth, and the ratio of line opacity to continuous opacity is held constant. As both of these assumptions play important roles in the line transfer, there is no guarantee that the resulting synthetic profiles are identical to actual profiles within a few percent—the entire amount of the expected effect. Thus, the accuracy of past reports of Zeeman broadening has been questioned, and all past quantitative measurements of magnetic fields on G and K dwarfs should be considered preliminary estimates. The above assumptions become increasingly suspect as one considers stronger lines; most previous work has used a line which is substantially weaker than the line considered here.

We present a Zeeman analysis which treats the line transfer of the Stokes parameters properly, i.e., in a full model atmo-

[1] Research reported herein is based on data collected at the Lick Observatory run by the University of California.

sphere, including all depth-dependent polarized opacities and atomic physics. We explore carefully the possibility that past claims of excess line broadening might be a result of poorly modeled broadening mechanisms or poorly modeled line transfer, but conclude that real fields have been measured. In addition, the theoretical approach presented in § II permits computation of intensity profiles at many points on the stellar disk thereby permitting calculation of flux profiles including, if desired, detailed treatment of macrobroadening and field morphology.

We have selected two Fe I lines in the near-infrared for the analysis of Zeeman broadening: λ8468.413 and λ7748.28. The first of these has been previously used in analyses of solar magnetic fields (thanks to D. Bruning for help in selecting these). They have very different Zeeman sensitivities, with Landé g-values of 2.5 and 1.1, respectively. Both are easily accessible with CCD detectors, permitting observations of high signal-to-noise and high resolution with standard astronomical spectrometers. Infrared lines offer an advantage over optical lines because of the λ^2 dependence of Zeeman splitting. This moves the circular Zeeman components further into the wings of the unsplit line that is formed in the field-free regions of a stellar atmosphere, thus providing significantly greater contrast for the magnetic signal. There are additional observational difficulties longward of the CCD range due to both detector and signal level problems, although Saar and Linsky (1985) have successfully observed at 2.2 μm. We have chosen both a sensitive line and an insensitive line to help differentiate between magnetic and nonmagnetic effects in the line formation.

II. THEORETICAL TREATMENT

Although Auer, Heasley, and House (1977) showed that results could be obtained with the Unno (1956) approximation for the Sun that are not inconsistent with other means of measuring the solar magnetic field, one has to wonder whether this is true for full flux profiles from a variety of other spectral types. The Unno approximation poorly treats several of the most important ingredients that go into making a line profile, including the $T(\tau)$ structure, the ratio of line to continuum opacity (η), and the line profile. In particular, the Planck function is assumed to be linear with continuum optical depth, η is assumed to be both constant and typically much smaller than is actually the case, and the line profile is taken to be Doppler rather than Voigt. This last point is particularly disturbing, since it is broadening in the line wings which is the signature of magnetic fields. Workers on cool stellar magnetic fields have shown that it is possible to find a set of parameters to generate profiles with this method that can be *scaled* to match observed stellar profiles. This is not the same as showing that the physical causes of the profiles are the same between theory and observation and has led to lingering doubts about the interpretation of the results.

a) A More Realistic Calculation

The equations which govern radiative transfer in the Stokes parameters are just like the ordinary transfer equation, but there are three of them and they are coupled to each other (Unno 1956). At the time Unno discussed them, no digital computers were available, and he made a clever analytic analysis to discover the basic behavior of the transfer. There is no longer any reason to resort to this approximation. We considered the possibility of using the usual Feautrier method on these coupled equations. It is easy to formulate the coupled solution, but unfortunately the crucial assumption of angular symmetry in the source function required by this method is not satisfied by transfer in the presence of magnetic fields that have arbitrary orientations. It may be possible to carry this out under the assumption of radial fields, which we actually adopt anyway for the study of stellar fields. Nonetheless, there is an even more straightforward approach which has full generality although it does not share the efficiency and stability of the Feautrier method. This is to simply follow the differential equations from the bottom of the atmosphere outward using a Runge-Kutta scheme. Since the bottom boundary conditions are known, and the stepsize can be made arbitrarily small (in principle) the coupled derivatives can be calculated at each step and applied to find the values of the variables at the next step. The only question is whether sufficient accuracy is computationally practical.

We adopt a second-order Runge-Kutta scheme with adaptive grid. The grid is chosen dynamically after the final optical depth scale is known at each frequency so there are at least a specified number of steps per each optical depth (our usual choice is three steps). The calculation is started at a specified continuum optical depth; typically a little greater than 10. A hermitic spline with some tension is used to interpolate all the needed quantities from the specified atmospheric grid onto the dynamic grid. As the atmosphere becomes optically thin, the grid relaxes until only the specified atmospheric points are used at small optical depths. At the bottom, the boundary conditions are that the intensity is equal to the Planck function, and the Stokes Q and V are zero. The Stokes U parameter is always zero in this formulation (Unno 1956) because it has no interaction with the other parameters. Derivatives are calculated and applied to get to the next step, new derivatives are calculated, and so on. We experimented with the grid size and starting point until no further changes in the results were noticed.

In order to make a flux integration from the intensity profiles, we have taken as our initial approach the standard Gaussian quadrature sum utilized for NLTE codes. The usual number of angles required is three; these are at approximately $\mu = 0.88$, 0.5, and 0.12. One advantage of the numerical solution is that one need not calculate some "average" angle for the magnetic field but can use the actual angle the field makes to the line of sight for each angle (where we have assumed the field to be perpendicular to the local surface). The depth grid is calculated separately for each line-of-sight angle, so that the slant path does not introduce larger stepsizes. We found that the scheme became unstable for grids much coarser than those used. The total number of grid points actually used is in the range of 100 for $\mu = 0.9$ and 350 for $\mu = 0.1$. We made a further economy in the wavelength grid actually used. The default wavelength steps are 0.01 or 0.015 Å until the line intensity reaches a value within 4% of the true continuum (which is previously computed). The spacing is then increased by 5 times, and the final profile interpolated back onto the finer grid afterward. The entire calculation takes typically a couple of minutes on a MicroVax II.

In order to do a realistic calculation, we used scaled solar models based on the HSRA, which is most appropriate for photospheric calculations. The detailed run of electron and particle densities is calculated in the standard way from the specified $T(m)$ structure. A microturbulent velocity of 0.8 km s^{-1} is assumed throughout the region of line formation. The

entire calculation assumed LTE (the NLTE effects are probably comparable to errors in the true atmosphere). The level populations of the iron lines were then found, and continuum and line optical depth scales computed. The main refinement for the calculation of magnetic fields is that there are separate optical depth scales for each of the Stokes parameters. The Zeeman transitions are computed from an LS coupling code based on Condon and Shortley (1970). This gives the relative intensities of the various Zeeman components at $\psi = 90°$ (where ψ is the angle between the field and the line of sight). The ψ dependence is explicitly accounted for in the Unno equations, however, so the Condon and Shortley intensities for the circularly polarized σ components must be corrected to their maximum values and then the sum of all angle-dependent intensities normalized to the total line opacity $\eta_0 \times \phi_\nu$. The line profile used is the Voigt function, with the appropriate frequency shift for any of the σ components. We checked that both the normalization and Runge-Kutta solution were working properly by computing a zero field case and comparing the results to those of an independent calculation using a preexisting LTE code with the same atmosphere.

Next we checked that the magnetic field profiles were being properly computed by comparing with the results from the original Unno (1956) paper. This necessitated removing all the atmospheric and line physics mentioned above and using constant property Milne-Eddington atmospheres (as previous investigators have done) and Doppler profiles. The difference is of course that we do not use the analytic solutions provided by Unno but employ the Runge-Kutta integration to calculate the profile. Our numerical results agreed with the analytic forms to better than 1%. As we tried to mimic the results for our realistic lines we noticed puzzling central "emission" bumps in the numerical calculations. These turn out to be predicted by the analytic formulae as well, but for values of η_0 in the hundreds to thousands (as discussed below). The realistic case does indeed contain such values over much of the atmosphere, but both Unno and subsequent investigators have not looked at values much over 10. We are satisfied that the numerical scheme can reproduce the unphysical cases properly and also compute correct physical results.

After this work was completed, we became aware of two preprints in which other authors have also decided to do a numerical solution to Stokes transfer. Landstreet (1988) has calculated profiles by assuming the Unno method to be accurate between each atmospheric grid point and integrating the result up through the atmosphere. With a sufficiently fine grid, this method becomes equivalent to the Runge-Kutta integration, but has additional accuracy and speed. If applied to usual model grids, however, there is a lingering problem with the assumed linear or constant atmospheric properties between grid points which may compromise the accuracy. This method is applied to the problem of magnetic Ap stars. For these the field strengths tend to be substantially larger than for late-type active stars, and the astronomical issues have more to do with the geometry of the field distribution on the stellar surface than its detection.

Another body of work by Rees, Murphy, and Durant (1988) and Lites *et al.* (1988) contains a more complete NLTE treatment of the line transfer applied to the measurement of all the Stokes parameters in the solar case. A more detailed analysis of some issues of the line formation appears there and more physics is included, appropriate to the quality of information available from the Sun compared to other stars. One of their conclusions is that, of all the approximations in the Unno approach, namely a linear source function, constant η, constant Doppler broadening, and constant (zero) collisional damping, it is the last one which generates the most severe errors. We have concentrated on the problem of measuring magnetic fields from stellar full-disk flux profiles in this paper, and our methods are perhaps more appropriate in this context.

b) Theoretical Results

In Table 1 are listed some of the atmospheric and line parameters for λ8468 in a K2 V stellar atmosphere (not all grid points actually used are tabulated). In particular, note the great variation and magnitude of the line to continuum opacity ratio η for these lines. This is not quite as bad as it seems since the contribution function is confined to a rather small part of the atmosphere, but it is clear that small ($\lesssim 10$) and constant η values are inappropriate. We tried to determine the best value

TABLE 1

ATMOSPHERIC PARAMETERS FOR λ8468 IN A K2 V STAR

log (Mass) (g cm^{-2})	Temp. (K)	τ_{5000}	τ_{8468}	η	Voigt a
−1.81E+00.....	4.09E+03	5.49E−05	3.71E−02	2.59E+03	1.07E−03
−1.61E+00.....	3.76E+03	8.67E−05	1.17E−01	2.49E+03	1.84E−03
−1.40E+00.....	3.67E+03	1.50E−04	3.05E−01	2.26E+03	3.05E−03
−1.21E+00.....	3.71E+03	2.76E−04	6.16E−01	1.77E+03	4.74E−03
−1.02E+00.....	3.78E+03	5.28E−04	1.11E+00	1.38E+03	7.10E−03
−8.54E−01.....	3.85E+03	1.03E−03	1.90E+00	1.09E+03	1.04E−02
−6.83E−01.....	3.92E+03	2.03E−03	3.17E+00	8.62E+02	1.51E−02
−5.17E−01.....	3.99E+03	4.04E−03	5.13E+00	6.817+02	2.18E−02
−3.51E−01.....	4.07E+03	8.03E−03	9.73E+00	7.95E+02	3.13E−02
−1.87E−01.....	4.15E+03	1.60E−02	1.25E+01	6.24E+02	4.49E−02
−2.32E−02.....	4.25E+03	3.19E−02	2.92E+01	4.83E+02	6.37E−02
1.35E−01.....	4.40E+03	6.37E−02	4.61E+01	3.63E+02	8.86E−02
2.90E−01.....	4.60E+03	1.27E−01	7.28E+01	2.60E+02	1.21E−01
4.43E−01.....	4.87E+03	2.54E−01	1.01E+02	1.67E+02	1.62E−01
5.98E−01.....	5.17E+03	5.06E−01	1.56E+02	9.61E+01	2.17E−01
7.52E−01.....	5.61E+03	1.01E+00	1.53E+02	4.17E+01	2.84E−01
8.78E−01.....	6.27E+03	2.06E+00	2.75E+02	1.261+01	3.37E−01
9.53E−01.....	7.05E+03	4.21E+00	2.46E+02	3.75E+00	3.54E−01
1.00E+00.....	7.65E+03	8.51E+00	2.59E+02	1.68E+00	3.65E−01
1.05E+00.....	8.10E+03	1.71E+01	2.78E+02	7.12E−01	3.85E−01

of η for the λ8468 line in the context of the Unno approximation by trying various values in our Unno code (with no magnetic field) and matching the observed solar profile. Note that the *scale* of the profile is arbitrary in the Unno approximation (i.e., the central intensity is a free parameter). We could achieve a fairly good match for $\eta = 80$ if we optimized a constant nonzero damping parameter.

We then tested the same profile parameters for the Unno case including a magnetic field against the results from a full numerical calculation for the Sun. For 1000 G we were somewhat surprised to find that the detailed wiggles in the line profile are still fairly well matched in the solar case. This means that the constant parameters and linear source function are not bad once proper values have been fixed. Using the same values for a different spectral type, however, requires an unphysical adjustment of the damping constant in order to fit the nonmagnetic profile. Furthermore, even after this adjustment has been made the profile is not a good fit to the real case once a magnetic field is introduced. Thus there is no guarantee that the nonphysical scaling procedure usually employed will allow accurate magnetic fields to be derived. It is apparent, though, that the errors introduced are not huge, and that such procedures are adequate as a rough approximation.

The intensity profiles themselves show some rather interesting variations as the magnetic field is turned up from zero. The linear polarization component of the Zeeman triplet might be expected to become more desaturated as the circular components move away from line center; these eventually become two additional distinct shifted absorption components. This happens eventually, but when the circular components are fairly mixed in the core (as is true for typical field values of interest), there is somewhat more complex behavior of the intensity profile. In particular, at around 1000 G for the λ8468 line a central "emission" bump appears. We originally thought this is due to the chromosphere present in the HSRA, but the same feature appears when we remove the rising part of the temperature structure, and the location of the contribution function argued against that explanation anyway. Furthermore, the analytic solutions with linear source function show the same feature for large values of η. Saar and Linsky (1985) also show complex profiles for some infrared lines.

This feature actually arises because the line center opacity is reduced compared to the outer core as the circular components are shifted away. When they are shifted too far, the line profile assumes the shape of the linear component which yields a normal looking absorption core. When they are close enough, however, their presence depresses the profile just off line center, leading to the pseudoemission bump at line center. This effect is enhanced at disk center, where the linear component has zero opacity. The behavior of the line profile in the HSRA (without its chromospheric section) as the magnetic field becomes stronger is illustrated in Figure 1. The center-to-limb behavior of these profiles is in the sense of decreasing the contrast of the profile variations relative to the (darker) continuum as one approaches the limb. Of course these profiles are only present before a flux integration, application of macrobroadening mechanisms, and the effects of instrumental resolution. Observed stellar profiles will not actually have these detailed shapes, but the shapes have some influence on the smooth profiles observed.

We now discuss the proper treatment of line blends. Our approach is to remove directly from the observations obvious blends which appear as simple absorption features in the far wings of the line (see § III*a*). Another method is to use a differ-

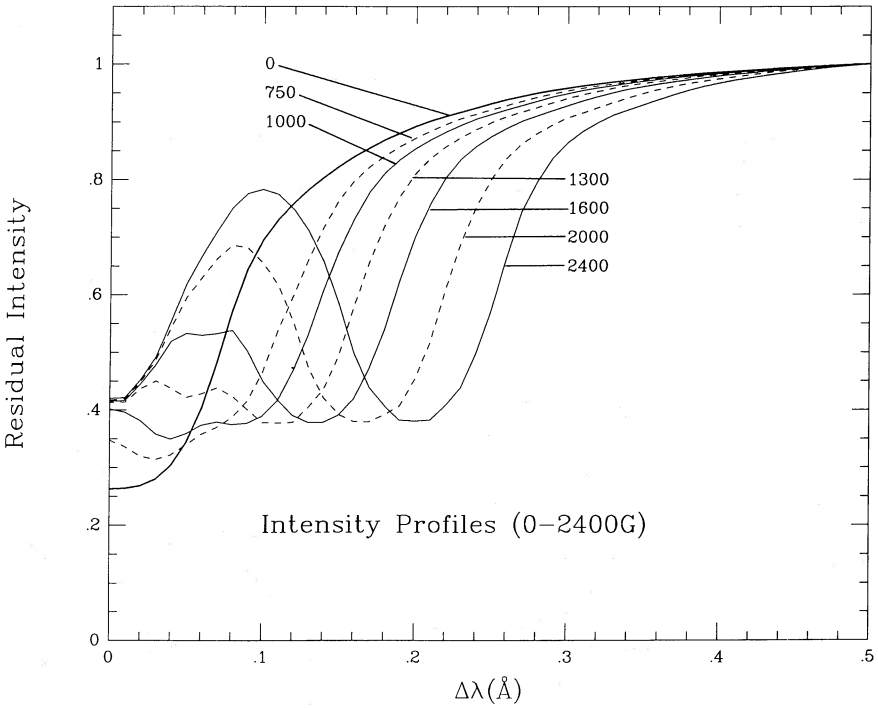

FIG. 1.—Theoretical intensity profiles for different magnetic field strengths. The HSRA atmosphere was used and the angle between the field and the line of sight was assumed arbitrarily to be 42°. Note that for field strengths less than 1000 G an apparent central reversal appears which is not due to the chromosphere (see text). Only for large field strengths does the intensity profile follow the shape of the underlying Zeeman absorption coefficient in a simple way.

ential approach in which a standard star is subtracted or divided out of the profile to be analyzed. Both of these are flawed in that the transfer in the blend is implicitly assumed to be independent of the transfer in the magnetic line, since the transfer in the magnetic line is clearly different for an active star compared to a nonmagnetic standard star. This is a dubious assumption when the blend lies in the same part of the line profile as the polarized component cores. This situation arises on the red side of the λ8468 line, where a Ti I feature mentioned in § III sits 0.05 Å longward of line center. This feature is weak, and not immediately obvious in observed spectra, but some asymmetry can sometimes be seen in the line. Fortunately it is a simple matter to include the opacity due to the blended line *depth by depth* in a numerical code.

We have explicitly included this line in the transfer problem with the *gf*-value from Kurucz and Peytremann (1975); we obtained an equivalent width of 16 mÅ in the Sun when the Fe I line is removed altogether. Its effect on equivalent width is of course smaller in the presence of the iron line and is around 5 mÅ. The blended profile has the expected behavior when no magnetic field is present, namely a depression of the red inner wing of the expected magnitude (although even here core saturation introduces a subtlety). For a field strength of 1500 G, however, the presence of the blend is much more obvious because it suppresses the pseudoemission feature altogether. Because of the interplay between the polarized components and the issue of saturation, it is not sufficient to treat such a blend *ex post facto*. In reality of course the blend might itself have Zeeman components (and this also presents no problem in principle). Fortunately in this case the blend is weak enough that large errors are not introduced even if it is not treated at all.

III. OBSERVATIONAL RESULTS AND ANALYSIS

We now apply the Zeeman line-transfer calculation to observed profiles to determine both the reliability of the theory and the magnetic fields on actual stars. The general approach adopted here is to observe two lines, one of low Zeeman sensitivity and the other with high sensitivity. The line of low Zeeman sensitivity provides information about the star itself, aside from the magnetic field, leaving the line of high Zeeman sensitivity to determine the magnetic field.

a) Observational Technique

Spectroscopic observations were made with the Lick Observatory coudé spectrograph on the 3 m telescope. Grating VII (900 g per mm) was used in second order with the 80 inch (2 m) camera and a TI CCD to yield a dispersion of 0.0332 Å per pixel at λ8468 and 0.0356 Å per pixel at λ7748. The slit width was 0".34, giving an instrumental profile with FWHM of 66 mÅ and 74 mÅ for the two lines, respectively. It is worth mentioning that grating VII is a Bausch and Lomb double diamond ruling, yielding slightly degraded resolution, and that it was used, by necessity, far from its second-order blaze wavelength of 6500 Å, resulting in lower efficiency and at large tilt angles which caused some vignetting. Observation times of about 30 minutes were required to achieve the typical signal-to-noise (S/N) ratio of 200 for a star of $V = 5$.

Here we report the results from a small stellar sample designed specifically to serve as diagnostics of the Zeeman analysis. The sample consists of the daytime sky (solar), ξ Boo A, a chromospherically active G8V star, and two K2 dwarfs, HD 166620 (chromospherically inactive), and ε Eri (chromospherically active). For each star, spectra were obtained at both lines, and typically several exposures were obtained during observing runs throughout 1986. All spectra were corrected for pixel-to-pixel sensitivity variations by dividing by a tungsten exposure and the wavelength scale is established with a thorium exposure. A small linear correction was applied to the slope of the stellar continuum to force it to be flat.

Extreme care was taken to remove blends in the two lines of interest. For λ8468.413 there is both a Mg I line that is 0.42 Å longward, having an equivalent width of about 10 mÅ and a telluric water line, 0.79 Å longward with equivalent width about 7 mÅ. As discussed earlier, there is also a Ti I line that is longward of λ8468 by 0.054 Å. Its equivalent width is unknown, but four other lines in the same multiplet are seen in the solar spectrum and have equivalent widths ranging from 5 mÅ to 21 mÅ (Moore, Minnaert, and Houtgast, 1966). The estimates of the *gf*-value of this Ti I line, given in Kurucz and Peytremann (1976) suggest that its equivalent width will be similar to the others in the multiplet. Thus, our approach to this line has been to include it in the line transfer calculation, as discussed in § II.

The Mg I blend was removed by using a neighboring Mg I line at λ8473.66 that has the same excitation as the blend and is always about 50% stronger in equivalent width. However, this reference Mg I line is so weak that its shape is poorly determined. We therefore used a nearby stronger Fe I line as an approximation to the shape of the reference Mg I line. We then simply subtracted an appropriately scaled version of the Fe I line from the original spectrum. We expect that this scheme reduces the blend to, at most, 1/10 of its original size, amounting to 1 mÅ equivalent width, and thus leaving contamination of no more than 1% of continuum. The telluric water feature was removed simply by using a scaled version of the nearby water line at λ8460.245 that was found to be consistently 10 times stronger. Note that all blends occur longward of λ8468 so that the red wing of the corrected observed profile is uncertain by perhaps several percent. The multiplet table (Moore 1972) shows no blends blueward of λ8468 so we believe the blueward wing to be considerably more reliable.

The other line of interest at λ7748.28 suffers from the encroachment of the blue wing of a neighboring Ni I line that is 0.61 Å longward. This wing is removed by simply subtracting the undisturbed red wing of the encroaching line from its blue wing. We expect errors in this procedure to be a fraction of a percent of the continuum height. After removal of the blends, both λ8468 and λ7748 were found to be symmetric at the level of the noise ($\sim\frac{1}{2}$%) of continuum. Thus it appears that the known blends have been removed adequately, and that unknown blends are not important.

The multiple spectra obtained for most stars were intercompared to search for variations resulting either from instrumental changes or from intrinsic stellar changes. No convincing variations were found at the level of 1% of the continuum. In particular, seven observations of ε Eri at λ8468 revealed no significant profile variations during the course of one year, suggesting that no dramatic changes took place in its surface magnetic-field characteristics. This result would seem to contradict reports that changes in field strength (Timothy, Joseph, and Linsky 1981; Marcy 1984) or changes in flux (Saar, Linsky and Duncan, 1986) are common in ε Eri.

b) Profile Analysis: Atomic and Stellar Parameters

The Zeeman line-transfer calculation has been used to examine various effects that determine emergent line shape in an effort to assess one's ability to convincingly detect the Zeeman effect. Within the context of an LTE calculation, the two atomic parameters that require scrutiny are the *gf*-value and the collisional broadening coefficient, C_6. Among the purely stellar parameters affecting line shape are abundance of the line-forming element, microturbulence, the thermodynamic structure of the atmosphere, macroturbulence, stellar rotation, and the magnetic field. By considering these effects, we attempted to determine whether an unambiguous detection of photospheric magnetic fields is really possible with line profiles in the spectral grasp of CCD detectors.

The answer to this question depends in part on the strength and surface coverage of fields found on actual stars. We have therefore chosen three stars, the Sun, HD 166620 (K2 V), and ϵ Eri (K2 V), as test cases to examine the various line-transfer effects mentioned above. The two K dwarfs were specifically chosen because of their different chromospheric characteristics. Epsilon Eri is well-known for its strong emission lines of chromospheric origin and rapid rotation, while HD 166620 has a rather long rotational period and low K-line emission. For all stars, both λ8468 and λ7748 were observed spectroscopically as described in § III*a*.

Atomic line parameters were determined as follows. As a first approximation, *gf*-values were taken from Kurucz and Peytremann (1975). These *gf*-values yielded synthesized solar profiles for λ8468 and λ7748 that were weaker by 10% than those observed for the Sun. Our observed equivalent widths for the Sun agree with those of Moore, Minnaert, and Houtgast (1966) to within a few percent. To resolve this discrepancy, we could have either adopted slightly larger *gf*-values or increased the classical collisional damping coefficient, C_6 of Unsöld (1955). Indeed, the *gf*-values reported by Blackwell *et al.* (1982) and Gurtovenko and Kostik (1982) for both lines are higher by about 0.2 dex than those of Kurucz and Peytremann. Since we were particularly interested in determining whether other broadening mechanisms could mimic Zeeman broadening, we have chosen to increase C_6 and retain the Kurucz and Peytremann *gf*-values. To do this, we simply multiply the classical collisional damping coefficient by 6 and 9 for λ8468 and λ7748, respectively. These values yielded excellent agreement between the calculated and observed equivalent widths. Attempts to increase C_6 further were found to be untenable because the wings of the theoretical lines become stronger than those observed, especially for the K dwarfs. It should be noted that other investigators have similarly found a need to augment C_6, e.g., Holweger (1971, 1972).

As a check of the validity of the LTE calculations, we attempted to synthesize the observed solar profiles by broadening the calculated profiles to account for solar rotation, macroturbulence, and instrumental profile. This is done by the standard convolution technique (Gray 1976) using a rotational broadening function, an exponential velocity distribution, and a Gaussian instrumental profile. Note that while an explicit disk integration would have been somewhat superior (Bruning 1984), our use of the low Landé *g*-line to determine macroturbulence implies that we are simply constructing an effective macroturbulent broadening function for later use with the high Landé *g*-line. The justification for this comes *ex post facto* from the fact that the low Landé *g*-line is fitted very well. The values used for the Sun were $v \sin i = 1.9$ km s^{-1}, and macroturbulent exponential half-width = 1.5 km s^{-1}, determined by trial and error. Figure 2 shows the theoretical and observed solar profiles for both λ8468 and λ7748. Clearly, both observed profiles are well fitted by the same macrobroadening functions.

c) The Detection of the Zeeman Effect

With the atomic parameters set, we applied the LTE line-transfer code to the two K dwarfs, HD 166620 and ϵ Eri. We constructed model atmospheres by scaling the temperatures of the HSRA solar model on a fixed continuum optical depth grid (Gray 1976), and recomputing the particle densities with the constraint of hydrostatic equilibrium. The abundance of iron is determined by trial and error for both stars by forcing a match between the theoretical equivalent width of the low Landé *g*-line and the observed equivalent width. The derived abundances were Fe/H = 2.15×10^{-5} for HD 166620, and Fe/H = 3.3×10^{-5} for ϵ Eri. As a consistency test, we then computed a theoretical profile for the high *g*-line in HD 166620 and found its equivalent width to be within $\frac{1}{2}$% of that observed, lending some confidence that the adopted K2 atmosphere and the line parameters work self-consistently for both lines.

We now broadened all theoretical profiles to account for rotation, macroturbulence, and instrumental profile, as described above. The value of $v \sin i$ for HD 166620 is not known, but the equatorial velocity was derived from the rotation period of 42 days as determined from Ca II K line periodicities (Noyes *et al.* 1984). Using a stellar radius appropriate for the spectral type and multiplying by the average value of sin *i*, one arrives at an approximate $v \sin i$ of 0.8 km s^{-1} for HD 166620. The macroturbulent half-width velocity for HD 166620 was then determined by fitting the observed low Landé *g*-line. The derived value is 1.0 km s^{-1}. The fit is quite good, as is seen in the upper left panel of Figure 3.

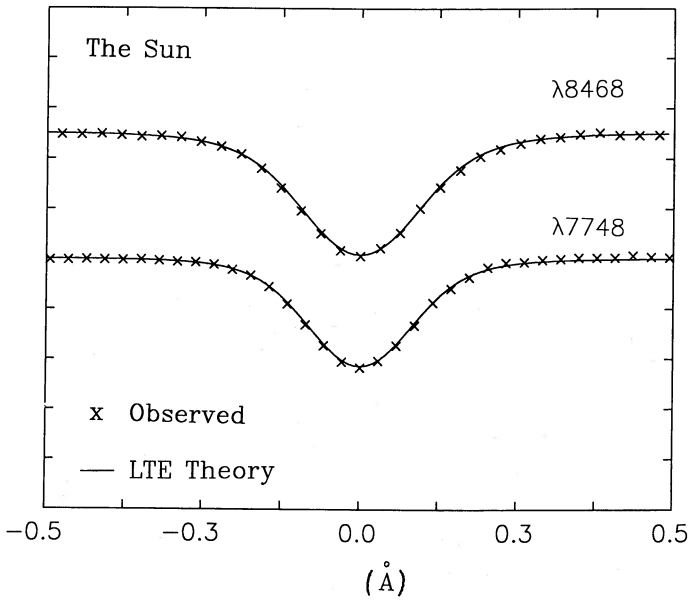

FIG. 2.—The observed and theoretical line profiles for the Sun. The top profile shows the best-fit to the Zeeman-sensitive line, λ8468, the bottom shows that for λ7748. The only free parameters were the collisional broadening coefficients for each line and a single macroturbulent velocity.

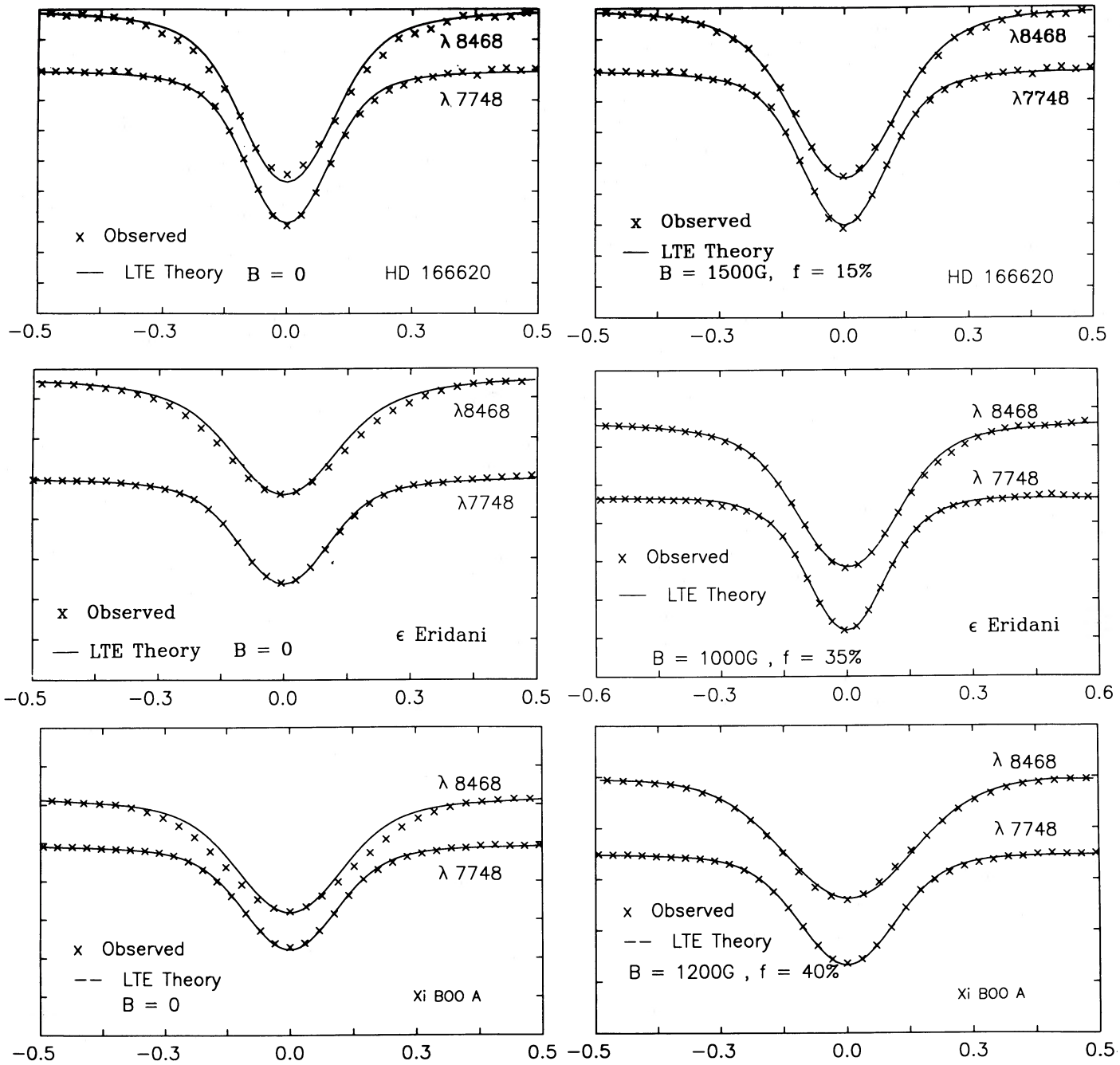

FIG. 3.—A comparison of the observed profiles to those computed theoretically for λ8468 (Zeeman sensitive) and λ7748 (Zeeman insensitive). The three stars shown are (from top to bottom): HD 166620, ϵ Eri, ξ Boo A. The panels on the left contain overlays of observed profiles on theoretical profiles constructed with no magnetic field. In these panels, note that the observed λ8468 profile is apparently broader than the theoretical profile, although the λ7748 profile is well fitted. The panels on the right show the fit obtained when a magnetic field is included in the theoretical computation. **B** is the field strength assumed where fields are present and *f* is the fraction of the stellar surface covered by fields.

Using this macroturbulent value, we calculated a theoretical λ8468 profile for HD 166620. Note that there are no free parameters in the construction of this profile. In particular, the observed profile is accepted without any scaling or correction for zero level and the theoretical profile is treated similarly. There could be a problem if scattered light in the spectrograph is not properly accounted for, but our comparisons with the solar atlas show this is not a major effect for us. This allows us to use the absolute central residual intensity in λ7748 to help fix the abundance, and in λ8468 to help determine the absolute magnetic field (in contrast to previous work where this information is scaled out). The resulting comparison between the theoretical and observed λ8468 is shown in the top left panel of Figure 3, and the fit is visibly not as good as for the low Landé *g*-line. The observed λ8468 line has visibly broader wings and a higher central intensity. One may suspect that this discrepancy in the fit to the high Landé *g*-line is due either to inaccuracies in the theoretical approach or to the presence of some other

broadening mechanism (e.g., magnetic field) which acts differently on the two lines. We explore these possibilities at the end of this section.

The procedure described above was then applied to ϵ Eri. The iron abundance having already been determined from the equivalent width of λ7748, the only unknown parameter is $v \sin i$. Smith (1983) finds that $v \sin i$ for ϵ Eri is 1 km s^{-1}, indicating that it is nearly pole-on judging from the observed rotation period from Noyes *et al.* (1984). Gray (1984*b*) finds a value of 2.2 km s^{-1}, despite his efforts to include Zeeman broadening. These authors agree, however, that the macroturbulence is greater, at 2.4 km s^{-1}. Since the rotational broadening will contribute little to the shape of the profile, we have arbitrarily adopted 1 km s^{-1} for $v \sin i$, with the knowledge that any small inaccuracies caused by this, will show up as a poor fit to the low Landé g-line. We also decided to adopt for ϵ Eri the macroturbulent velocity used for HD 166620, since the spectral types are the same. Thus, there are no free parameters in the construction of the theoretical profile for λ7748 of ϵ Eri, with the exception of the use of the observed equivalent width to determine Fe/H. The middle left panel of Figure 3 shows this theoretical profile plotted over that observed. The fit is visibly very good and suggests again that the line-transfer code along with the adopted line parameters and stellar parameters reliably synthesize profiles without need for ad hoc adjustments.

The computation of the high Landé g-line for ϵ Eri is carried out with absolutely *no free parameters*, i.e., the same stellar parameters used for the low Landé g-line are used here. The resulting theoretical profile for λ8468 is shown plotted over the observed profile in the middle panel of Figure 3. It is clear that the observed profile has stronger wings than the theoretical profile, which was computed assuming no magnetic field. This discrepancy is far greater than any found in the previous tests of the theory. We are compelled to conclude that the high Landé g-line has been selectively affected by some broadening mechanism, presumably the Zeeman effect.

d) Determination of the Magnetic Field

We now employ the LTE code to determine whether the introduction of magnetic fields can adequately explain the shape of the observed profiles in ϵ Eri. We assume that the observed line profiles may be synthesized by constructing the weighted sum of theoretical profiles from magnetic and nonmagnetic regions. Both the low Landé g- and the high Landé g-line must simultaneously be fitted with the same stellar parameters, including magnetic field. Since the Zeeman effect broadens the line absorption coefficient, the presence of magnetic fields typically increases equivalent widths. We are therefore forced to lower the Fe abundance in ϵ Eri in order to construct a theoretical profile for the low Landé g-line that has the observed equivalent width. Thus, an iterative procedure is required in which the observed high Landé g-line is used to obtain the magnetic field strength and covering fraction. Then, the abundance is recomputed by forcing the theoretical equivalent width of the low Landé g-line (with a magnetic field) to match that of the observed line. Fortunately the equivalent width of this line is not greatly changed by the field (which is why it was chosen in the first place). Finally, the theoretical profile without a magnetic field is added to theoretical profiles with different field strengths and weighting factors to synthesize a final profile that includes the effect of magnetic surface filling factor. This procedure has been carried out for ϵ Eri, and the resulting theoretical profiles are plotted over the observed profiles in middle right panel of Figure 3. There is obviously a good fit.

The final derived magnetic field strength for ϵ Eri is 1000 G, covering 35% of the star. Recall that the observed profiles are actually averages of seven separate observations obtained over the course of several months in 1986, so the derived fields can be considered time averages. Note also that we assume the atmosphere in magnetic regions to be identical to that in magnetic-free regions; clearly not the case on the Sun. In addition, we do not take into account possible velocity field differences in the two regions, as are observed on the Sun (see, e.g., Title, Tarbell, and Topka 1987).

We have also applied the above procedure to ξ Boo A. We adopted a gravity from the mass relation given in Noyes *et al.* (1984) and the radius given in Mihalas and Binney (1981). The value of $v \sin i$, 2.5 km s^{-1} is taken from Soderblom (1981). We required an abundance Fe/H = 2.6×10^{-5}, and a macroturbulent exponential half-width of 1.6 km s^{-1} to obtain a good fit with the low Landé g-line. The resulting best-fit values for the magnetic field were: **B** of 1200 G covering 40% of the star. The bottom panels of Figure 3 show the fits for both the low g and high g-line. Note that the λ8468 profile is asymmetric in the core, perhaps due to differential velocities in the magnetic regions.

We have made only qualitative estimates of the internal uncertainties in the magnetic field values. By constructing theoretical profiles with different assumed values for field strength and covering factor we visually assessed their "goodness of fit" to the observed profiles. This crude approach showed that field strengths were uncertain by about 300 G and surface covering fractions were uncertain by about one-fifth of the derived value. Figure 4, for example, shows that if one wanted to fit the ξ Boo A high g-line with 1500 G instead of 1200 G, a lower covering factor of 30% would be required. The resulting theoretical profile is a slightly poorer fit than that obtained with the best-fit field values. As discussed below, the true uncertainties owing to our lack of knowledge of the atmospheric physics are probably more important than the formal errors in a fit.

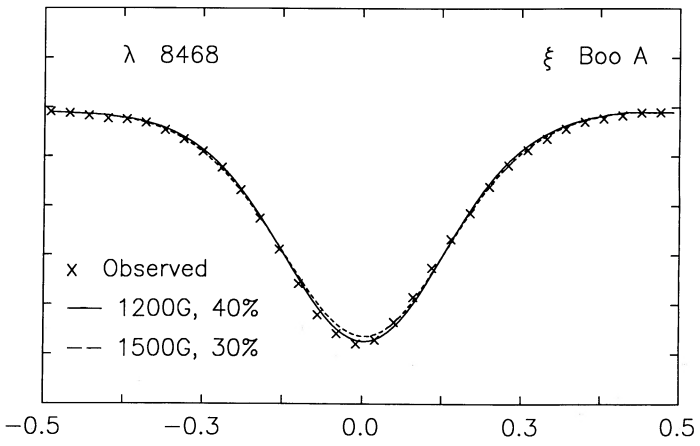

FIG. 4.—Two theoretical profiles representing different magnetic field characteristics overlaid on the observed profile of ξ Boo A. The solid line represents the profile for a field of 1200 G covering 40% of the surface, while the dashed line represents that for 1500 G covering 30%. The latter case shows the best-fit obtainable for **B** = 1500 G. The tics are at intervals of 10% of the continuum.

To demonstrate the effect that the filling factor and field strength have on a profile, we show in Figure 5*a* the ratio between the λ8468 and λ7748 lines for our best-fit case in ϵ Eri and for values near those. This shows that kilogauss fields can produce changes in observed λ8468 profiles of 5%–10%. In this case the filling factor changes primarily the amplitude of the bumps in the ratio spectrum relative to the central dip, while the field strength changes the separation of the bumps and the depth of the central dip. The central dip is independent of filling factor in this case because the central intensity of the 1000 G flux profile is nearly the same as without a field (Fig. 5*b*). Of course both parameters are varied when an actual fit is being made. Nonetheless, the adjustment is more sensitive to the field strength, which must be reasonably close before filling factor can be used to tune up the profile. High strength fields yield profiles with shallow cores and very broad wings (Fig. 5*b*), so they cannot arbitrarily be mixed in with small filling factors and still yield a good match over a whole line profile. An objective procedure for making the best profile fit is discussed in § IV.

Even without such a procedure it is clear in Figure 2 that the observed λ8468 for HD 166620 is not well fitted by a theoretical profile constructed with **B** = 0. An attempt to better fit this observed profile with synthetic profiles of various magnetic field characteristics yields **B** = 1500 G, and $f = 15\%$, as shown in the upper right panel of Figure 3. This fit is carried out using the stellar parameters for HD 166620 given above. A final tabulation of all stellar parameters used in the fits for all four stars is given in Table 2.

TABLE 2

FINAL DERIVED STELLAR PARAMETERS

Star	**B** (G)	f %	Fe/H ($\times 10^{-5}$)	$V_{\rm Macroturbulent}$ (km s^{-1})	$v \sin i$ (km s^{-1})
Sun	...	0	3.0	1.5	1.9
HD 166620	1500	15	2.15	1.0	0.8
ϵ ERi	1000	35	3.3	1.0	1.0
ξ Boo	1200	40	2.6	1.6	2.5

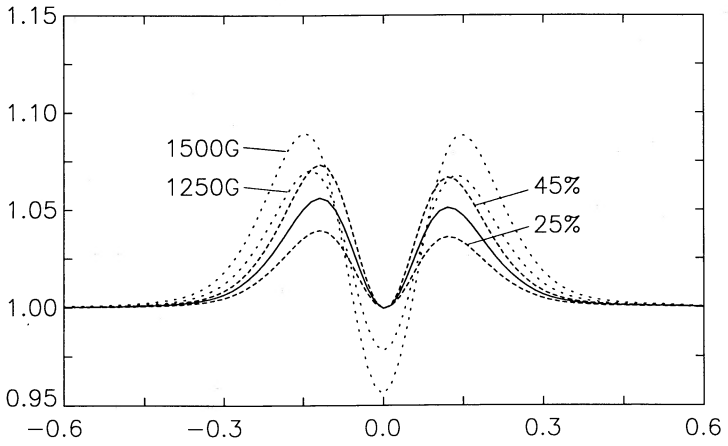

FIG. 5*a*

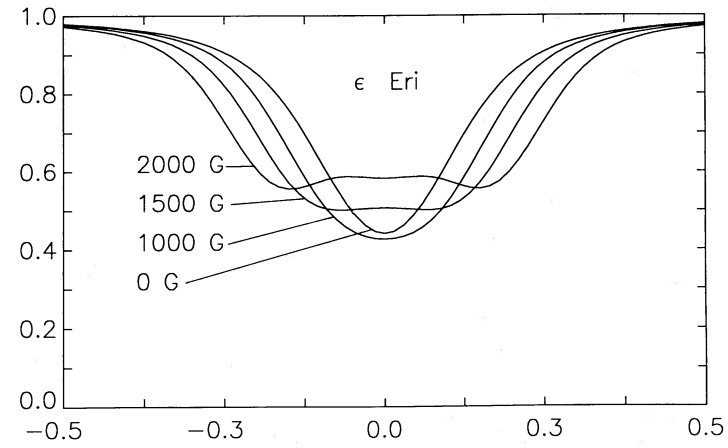

FIG. 5*b*

FIG. 5.—Demonstration of the effects of field strength and the fraction of the surface covered by fields for the star ϵ Eri. (*a*) shows the ratio between the λ8468 and λ7748 profiles for different assumed magnetic field characteristics. The ratio of the profiles that best fit those observed is shown in the solid line, representing **B** = 1000 G and a stellar surface coverage, f, of 35%. The lines marked 1500 G and 1250 G show what happens if **B** changes but f remains at 35%. Similarly, the lines marked 45% and 25% show the effects of changing f but retaining **B** = 1000 G. Note that changes in the magnetic field of these amounts cause detectable changes in the profiles. (*b*) shows the theoretical flux profiles for different assumed field strengths, assuming $f = 100\%$. Note that the central intensity is not a monotonic function of field strength.

It is somewhat disturbing that a star with such a slow rotation period and weak Ca II K emission as HD 166620 has a detectable magnetic field. Is this telling us something about K dwarfs compared with G dwarfs, or is it a deficiency of the analysis? At the urging of L. Hartmann, we attempted to negate the field detection by redoing our analysis with the bias that no field should be found for this null star. This entails forgetting about the atomic line parameters we found using the Sun as a null star, and trying to find values for the common abundance, individual oscillator strengths, and collisional damping coefficients which reproduce the observed lines in HD 166620 without any magnetic field. Because we once again have independent choices to make for each line, we were able to make fits for this star which looked reasonable (though not as good as when using a magnetic field) but λ8468 required a value for C_6 of 50 times the Unsöld value. Then, to match the observed equivalent width of λ8468, we were forced to adopt a value of gf that is 0.4 dex below the Blackwell *et al.* (1982) value. Neither value for these parameters is very reasonable. They can be firmly rejected because their use with the solar atmosphere does not allow a fit to the observed solar λ8468 line. It therefore appears that there is some anomalous broadening of the λ8468 line in HD 166620 which is not present in the λ7748 line, and the conclusion that there is a magnetic field on this star is reasonable from an observational point of view. We have observations of several other "null" K stars which can be used to determine whether the simplest expectations from dynamo theory are being violated.

A comparison of our field determinations with other investigations can be made, although our method is substantially more physical than previous techniques. For ϵ Eri, published values of $\mathbf{B}(f)^{1/2}$ are less than 400 (Saar 1988), 320 (Saar, Linsky, and Duncan 1986), 590 (this work), 950 (Marcy 1984), and 1040 (Gray 1984*a*). For ξ Boo A published values are less than 500 (Gondoin, Giampapa, and Bookbinder 1985), 760 (this work), 900 (Marcy 1984), 1080 (S. Saar, private communication 1987), 1440 (Robinson, Worden, and Harvey 1980). We have some doubt that these values represent real variations, based on our unvarying spectra taken over one year and on the obvious differences in the data quality and analysis techniques in these works. It will be important to follow up with this improved technique on other high-quality observations at other epochs and wavelengths.

IV. DISCUSSION AND SUMMARY

a) Uncertainties

We have not carried out a quantitative estimate of the errors in our derived magnetic field estimates. The reader may refer to Saar (1988*a*) for a thorough discussion of some of the possible errors. We feel that the dominant uncertainty in this analysis derives not from the noise in the spectra, but from our lack of knowledge of the physics of stellar atmospheres. In particular, we simply do not know the thermodynamic or hydrodynamic structure of the magnetic regions in active stars. Since the fraction of the stellar surface covered by fields is rather large for these stars, we really do not understand the nonmagnetic regions of the atmosphere either, as even the observed colors of such stars may be affected by the plagelike regions and spots. However, our ability to adequately synthesize the low Landé g-line suggests that our ignorance of the atmospheric physics can be overcome somewhat by choosing values of turbulence and Fe abundance which are undoubtedly slightly different from reality. Since such fixes in the theoretical calculations act similarly on both the low Landé g-line and the high Landé g-line, we must conclude that the resulting apparent Zeeman broadening in the observed high Landé g-line is only slightly affected by our ignorance of the stellar physics.

To be conservative, we investigated whether there is a possibility that conventional broadening sources could be responsible for the observed shapes of λ8468 in ϵ Eri and ξ Boo A. An attempt was made to fit both the low Landé g-line and the high Landé g-line with a variety of combinations of assumed values for gf, v sin i, macroturbulence, Fe abundance, and C_6. None of these came close to providing simultaneous fits. In particular, magnetic field-free models with increased rotation and macroturbulence (and suitable abundance changes) can be found such that a reasonable fit is achieved with the observed high Landé g-line. But then the low Landé g-line is extremely poorly fitted. More interestingly, a strong effort was made to determine whether differential collisional broadening between the two lines could account for the observed enhanced broadening of λ8468. By increasing the value of C_6 to 20 times its conventional value (instead of only 6 times), the theoretical λ8468 line for ϵ Eri developed wings that were closest to those observed, but extended far beyond those in the observed profile. At the same time, the core of the theoretical profile is not as broad as that observed. Evidently, the convolution of an enhanced Lorentzian with the line absorption coefficient does a poor job of fitting the observed profile and cannot account for the observed broadening on active stars.

There are now a number of convincing arguments against the objections that have been raised regarding the interpretation of broadening in high Landé g-lines as due to magnetic fields, or the values of magnetic flux deduced. The effects of both line saturation and blending have now been treated including the important physical effects. Perhaps the most convincing evidence is that with such a proper treatment, the observational profiles can be matched to a high degree of accuracy without any adjustment or scaling of the observed profiles or ad hoc adjustment of physical parameters which have been set from the Sun. The profiles fit in detail in the Doppler core, the far wings, and the inner wings where the field has its greatest effect. By using unscaled profiles one has an additional check on the field parameters derived since the core intensity must now also fit. The rather large filling factors found must now be taken more seriously, and their implications for stellar activity and dynamo theories explored.

b) Summary of the Improved Methodology

To recap our entire procedure, we first compute line profiles with an LTE code and physical model atmosphere appropriate to the effective temperature and gravity of the star under study. There are several approaches possible in this computation; we have used a simple Runge-Kutta scheme here. This makes it particularly easy to treat several angles on the stellar disk and to include blended lines explicitly if desired. The line parameters are all depth dependent, and based on the relevant atomic parameters. When these are uncertain, they are determined from the appearance of solar lines. Note that in principle these need only be determined once for each line that is used in the analysis. The only parameters remaining to be determined for a star are the abundance and macrobroadening parameters, and these are fixed by the magnetically insensitive line. The

final determination of the magnetic field from a sensitive line therefore is done *without free parameters.*

Our observations were made of two neutral iron lines which are near the long wavelength end of the CCD spectral range to take full advantage of these well-used detectors and the λ^2 dependence of Zeeman broadening. Obvious blends exist in the red wings of the chosen lines and can be removed from the observations, or they can be included in the theoretical treatment. As discussed below, one can use a fitting procedure which is relatively insensitive to the presence of blends in any case. Because the fields on cool stars are not very strong, the effect to be detected is rather subtle, and line intensities at every point in the profile should be known to an accuracy of 1%. The observations must therefore be of high quality; a signal-to-noise of at least 200 is desirable, and less than 100 is unacceptable. The continuum should be well determined, and the scattered light level must be assessed. The profiles are used as they are, without arbitrary scaling or renormalization.

Although the fitting used in this preliminary work is more qualitative than finally desirable, we are working on a method which should give good objective measures of the field strength and filling factor, assess the formal error in the estimates, and be insensitive to the presence of unremoved blends. The usual procedure has been to make a χ^2 analysis using the analytic Unno profiles scaled to observations. Instead, one must compute a grid of profiles for each model atmosphere in both lines and for a set of field strengths. The strengths can be sampled every 250–500 G and profiles can be computed from weighted averages for intermediate values. In less than an hour of computing time a full grid for a given spectral type can be generated. The macrobroadening specific to a given star can be applied to the profiles from this grid. Nonmagnetic profiles are then mixed with magnetic profiles with different weightings for the determination of the filling factor. This must be done for a variety of proposed field strengths.

The comparison between the test grid and the observations should be made to *maximize the number* of observed points which *fall within a specified distance* (point by point) of each theoretical profile. The use of a χ^2 statistic gives undue weight to observational points which lie well off the expected profile (such as in blends or noise spikes) since it is this distance squared which enters in the quantity to be minimized. The best-fit profile from such a procedure is one which wanders partway between clean observational points and discrepant points to minimize the total error. Our qualitative fitting procedure essentially ignored blends, since we knew that the theoretical profile should not be expected to match points within them. One should be trying to assess how well the observational shape matches the theoretical shape, not just trying to minimize the total discrepancy. By maximizing the number of points which fit well, one obtains the theoretical profile which best mimics the observations while ignoring clearly discrepant points, since profiles which pass near to discrepant points miss most of the rest of the observed points. One can finally hone the fit by examining the χ^2 statistic for only points which are counted as near the theoretical profiles if there are several fits with nearly the same number of points which lie within the rejection threshold.

The window within which a theoretical and observational point are considered to match must be adjusted based on the signal-to-noise of the observations. In computing the goodness of fit, one can give extra weight to the blue wings for the lines we have chosen since they are believed to be clean of blends, are not modified by our attempts to remove blends, and therefore should match theoretical curves more closely. One can plot the goodness-of-fit parameter as a function of field strength and filling factor, learning both where it is maximized and how uniquely determined the values of these two derived quantities really are. One obtains thereby an objective measure of both the values of the parameters and the formal uncertainty in those values. The entire procedure of this section should be used in the future with high-quality observations to place the study of stellar magnetic fields on more solid ground.

Several additional improvements should be attempted in future magnetic field measurements. A full disk integration can be carried out that uses intensity profiles from a larger number of disk locations, thereby enabling both a proper treatment of macrobroadening (Bruning 1984) and more detailed modeling of the field morphology. Second and more important, future attempts should explore the use of two-component stellar surfaces; including separate atmospheres for the magnetic and nonmagnetic regions. This may be done, as a first approximation, by scaling empirical solar atmospheres in quiet and facular regions, or by appropriately using empirically determined average atmospheres for active and inactive stars. Such modeling attempts should also explore the effects of velocity fields in the magnetic regions, especially with regard to the formation of line asymmetries when they are observed. Finally, the precision of future magnetic field work can be enhanced if more lines are used in the analysis. This will diminish errors that result from blends and uncertain line parameters. It would of course be desirable to collect the observations of all lines at the same time. Finally, it is also desirable to concurrently collect diagnostics of chromospheric activity for direct comparison with the magnetic field observations, since both the field and the activity can be expected to vary and it is of prime importance to study their variations together.

We would like to acknowledge helpful conversations with S. Saar, D. Bruning, and L. Hartmann. This work was supported, in part, by NSF grants AST 86-03979 to G. M. and AST 84-14811 to G. B. Observations at the Lick Observatory are supported in part by NSF block grant AST 86-14510 to the University of California.

REFERENCES

Auer, L. H., Heasley, J. N., and House, L. L. 1977, *Solar Phys.*, **55**, 47.
Basri, G. 1987, *Ap. J.*, **316**, 377.
Blackwell, D. E., Petford, A. D., Shallis, M. J., and Simmons, G. J. 1982, *M.N.R.A.S.*, **199**, 43.
Bruning, D. H. 1984, *Ap. J.*, **281**, 830.
Condon, E. U., and Shortley, G. H. 1970, *The Theory of Atomic Spectra* (London: Cambridge University Press).
Gondoin, P., Giampapa, M. S., and Bookbinder, J. A. 1985, *Ap. J.*, **297**, 710.
Gray, D. F. 1976, *The Observation and Analysis of Stellar Photospheres* (NY: Wiley).
———. 1984*a*, *Ap. J.*, **277**, 640.
Gray, D. F. 1984*b*, *Ap. J.*, **281**, 719.
Gurtovenko, E. A., and Kostik, R. I. 1982, *Astr. Ap. Suppl.*, **47**, 193.
Holweger, H. 1971, *Astr. Ap.*, **10**, 128.
———. 1972, *Solar Phys.*, **25**, 14.
Kurucz, R. L., and Peytremann, E. 1975, *A Table of gf-Values* (*Smithsonian Ap. Obs. Spec. Rept.* 362).
Landstreet, J. D. 1988, preprint.
Lites, B. W., Skumanich, A., Rees, D. E., and Murphy, G. A. 1988, preprint.
Marcy, G. W. 1984, *Ap. J.*, **276**, 286.
Mihalas, D., and Binney, J. 1981, *Galactic Astronomy* (San Francisco: Freeman).

Moore, C. E. 1972, *A Multiplet Table of Astrophysical Interest* (NSRDS-NBS 40).
Moore, C. E., Minnaert, M. G. J., and Houtgast, J. 1966, *The Solar Spectrum 2935 Å to 8770 Å* (*NBS Monog.* 61).
Noyes, R. W., Hartmann, L., Baliunas, S. L., Duncan, D. K., and Vaughan, A. H. 1984, *Ap. J.*, **279**, 763.
Rees, D. E., Murphy, G. A., and Durant, C. J. 1988, preprint.
Robinson, R. D. 1980, *Ap. J.*, **239**, 961.
Robinson, R. D., Worden, S. P., and Harvey, J. W. 1980, *Ap. J.* (*Letters*), **236**, L155.
Rutten, R. G. M., and Schrijver, C. J. 1987, *Astr. Ap.*, **177**, 155.
Saar, S. 1988*a*, *Ap. J.*, **324**, 441.
———. 1988*b*, IAU Symposium No. 132, preprint.
Saar, S. H., and Linsky, J. L. 1985, *Ap. J.* (*Letters*), **299**, L47.
Saar, S., Linsky, J. L., and Duncan, D. K. 1986, in *Fourth Cambridge Workshop on Cool Stars, Stellar Systems, and the Sun*, ed. M. Zeilik and D. Gibson (NY: Springer-Verlag), p. 275.
Simon, T., and Fekel, F. C., Jr. 1987, *Ap. J.*, **316**, 434.
Smith, M. A. 1983, *Pub. A.S.P.*, **95**, 268.
Soderblom, D. R. 1981, *Ap. J.*, **263**, 239.
Timothy, J. G., Joseph, C. L., and Linsky, J. L. 1981, *Bull. AAS*, **13**, 828.
Title, A., Tarbell, T. D., and Topka, K. A. 1987, *Ap. J.*, **317**, 892.
Unno, W. 1956, *Pub. Astr. Soc. Japan*, **8**, 108.
Unsöld, A. 1955, *Physik der Sternatmospharen* (2d ed.; NY: Springer-Verlag).

GIBOR BASRI: Department of Astronomy, University of California, Berkeley, CA 94720

GEOFFREY W. MARCY: Department of Physics and Astronomy, San Francisco State University, San Francisco, CA 94132